

Study of Extragalactic Supernova Remnants

Maria Kopsacheili

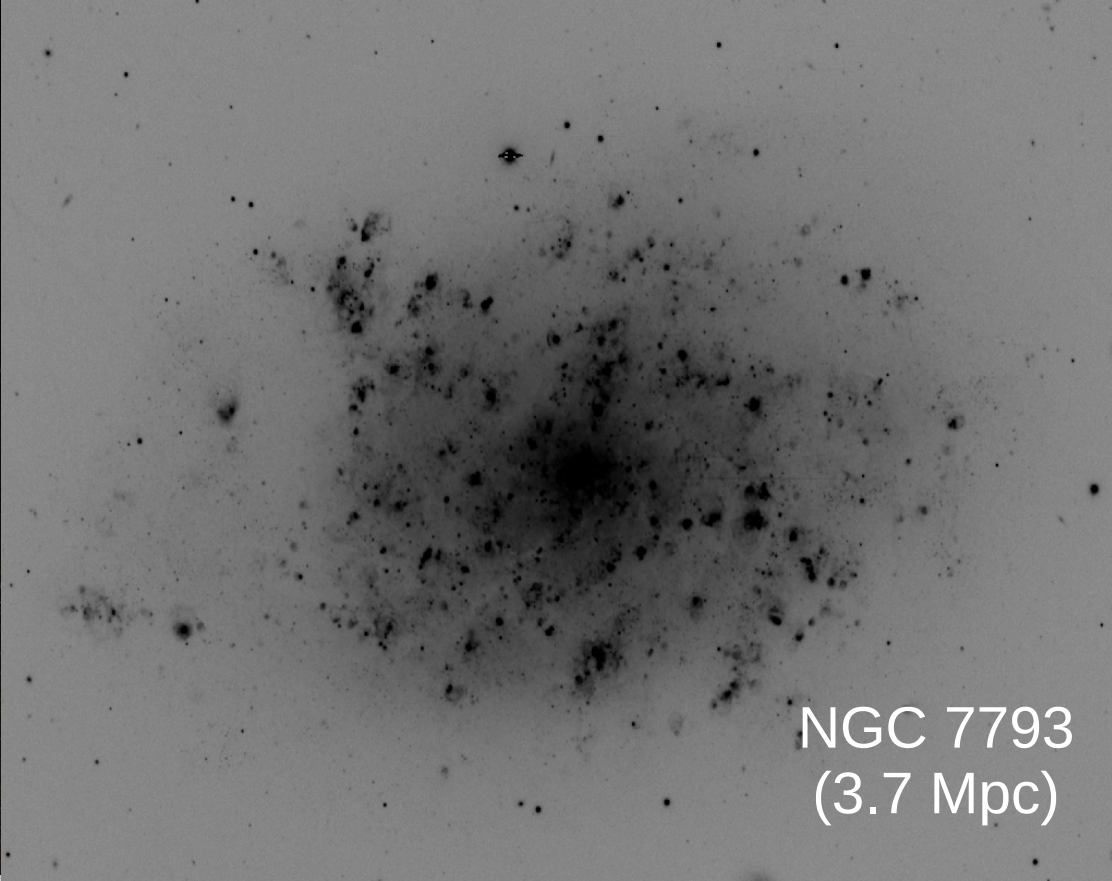
University of Crete/FORTH

Andreas Zezas
Ioanna Leonidaki
Panos Boumis

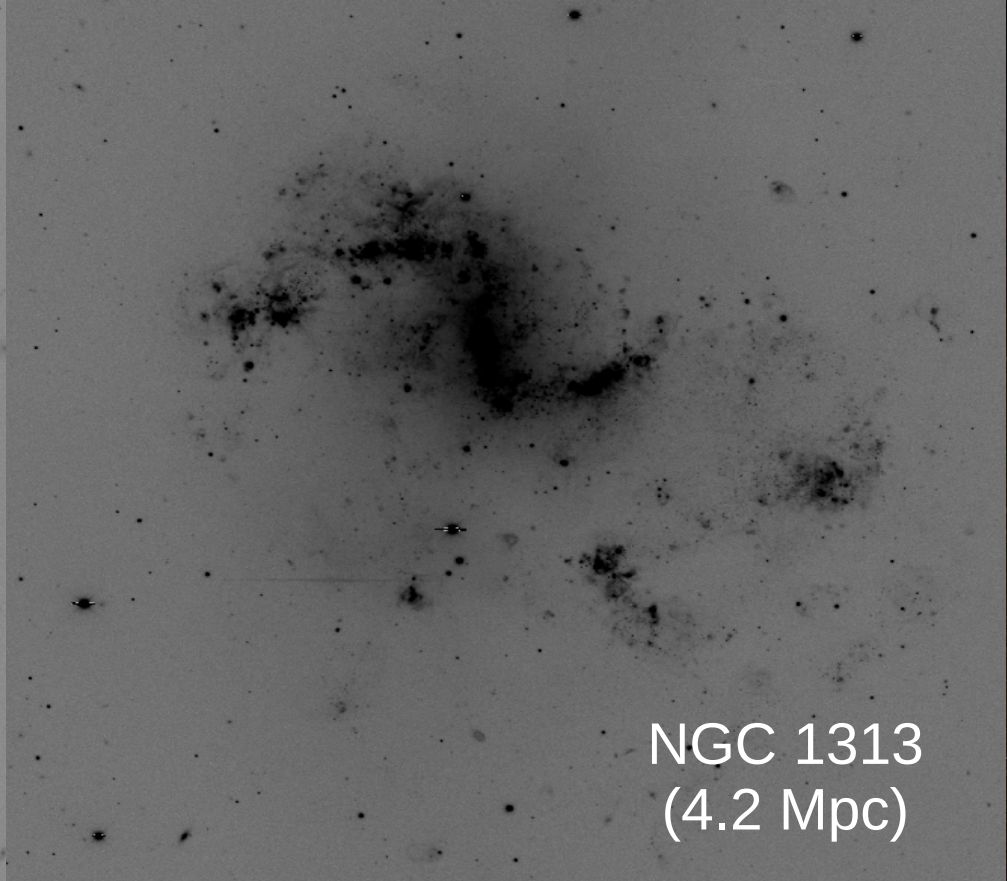


UNIVERSITY
OF CRETE

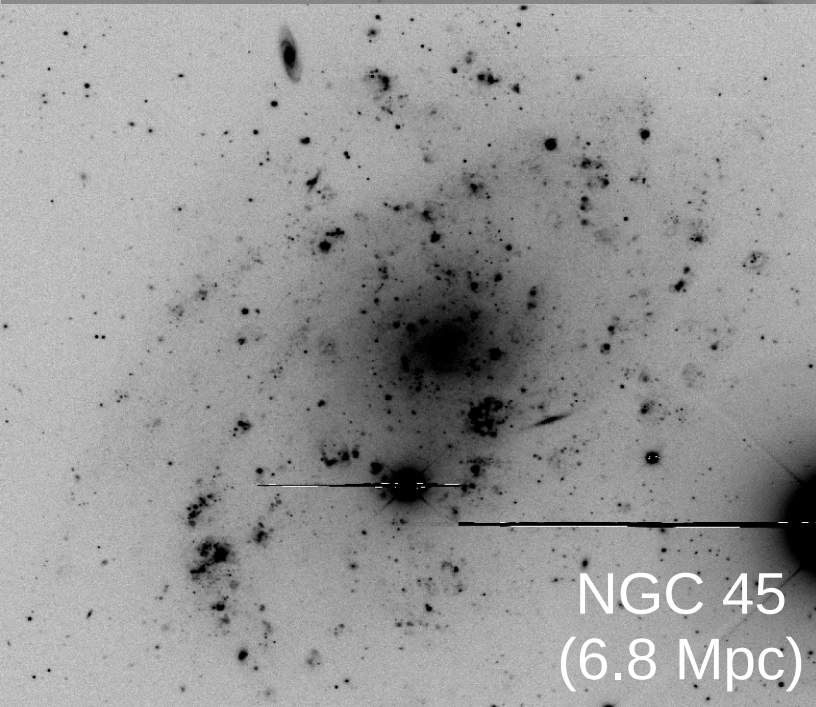




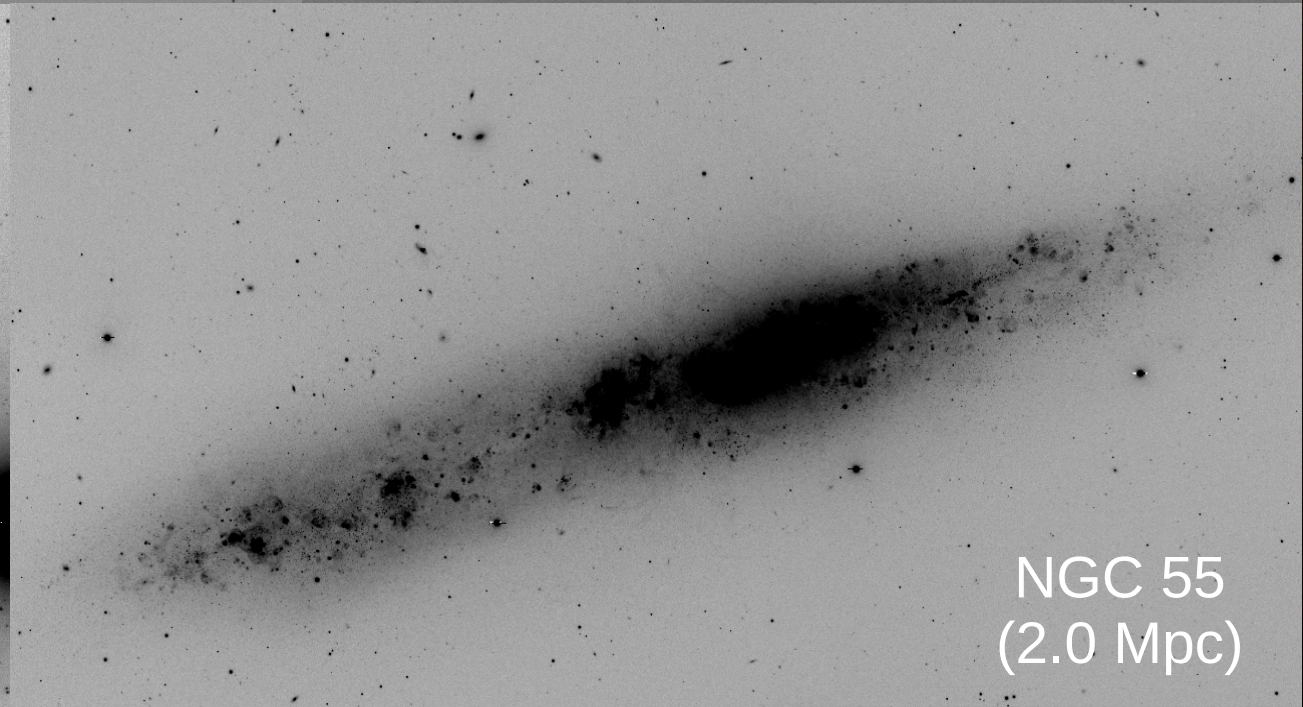
NGC 7793
(3.7 Mpc)



NGC 1313
(4.2 Mpc)



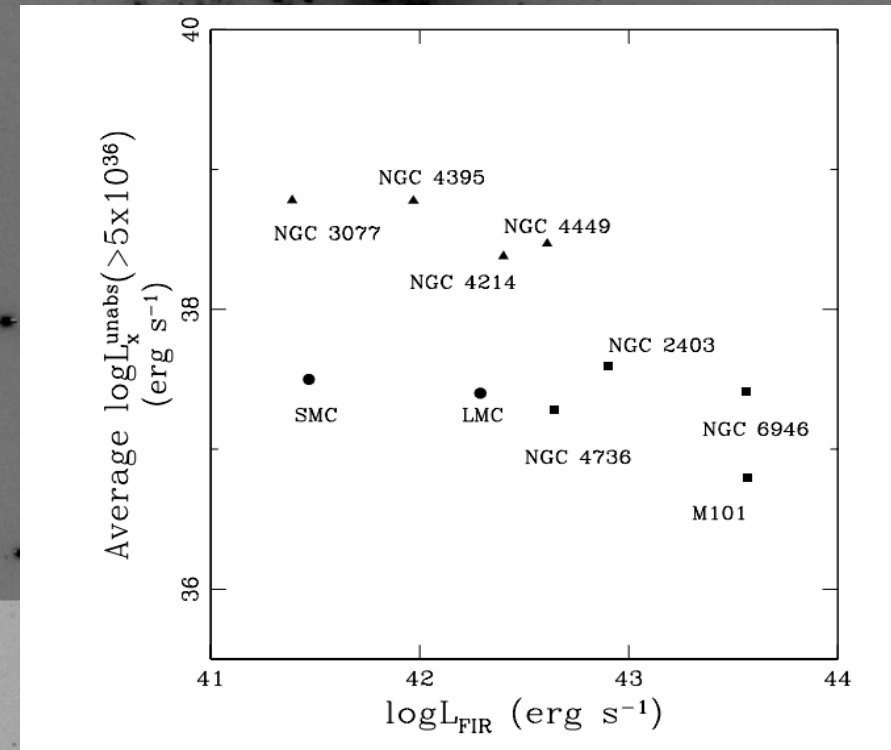
NGC 45
(6.8 Mpc)



NGC 55
(2.0 Mpc)

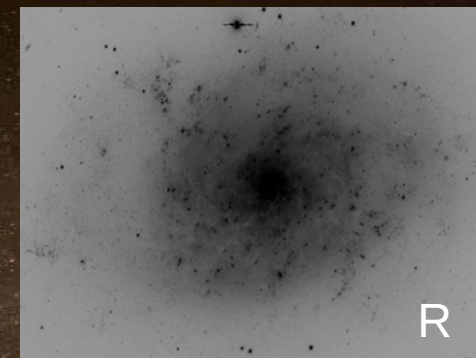
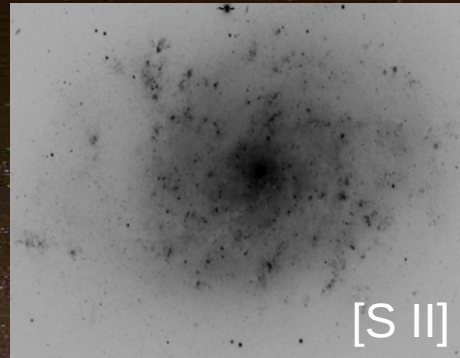
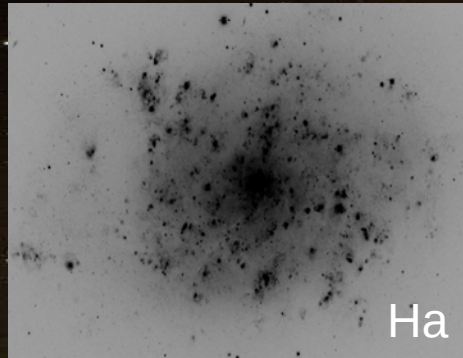
Galaxy sample

- Spiral galaxies (already irregular galaxies, Leonidaki et al., 2010; 2013)
- Nearby galaxies
- Face on or very “transparent” galaxies
- X-ray data available
 - ◇ Observations with Blanco 4m telescope at CTIO, in Chile



Leonidaki et al, 2010

Detection - Photometry - Flux calibration

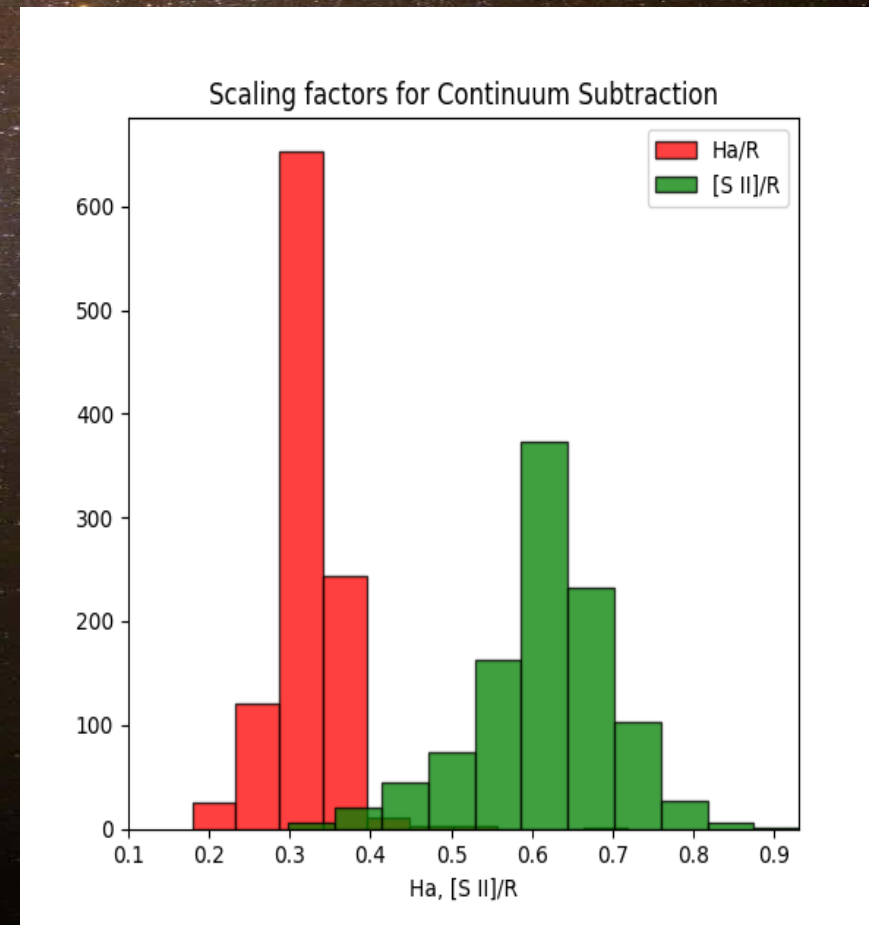


Detection on Ha+[S II] image (SExtractor)

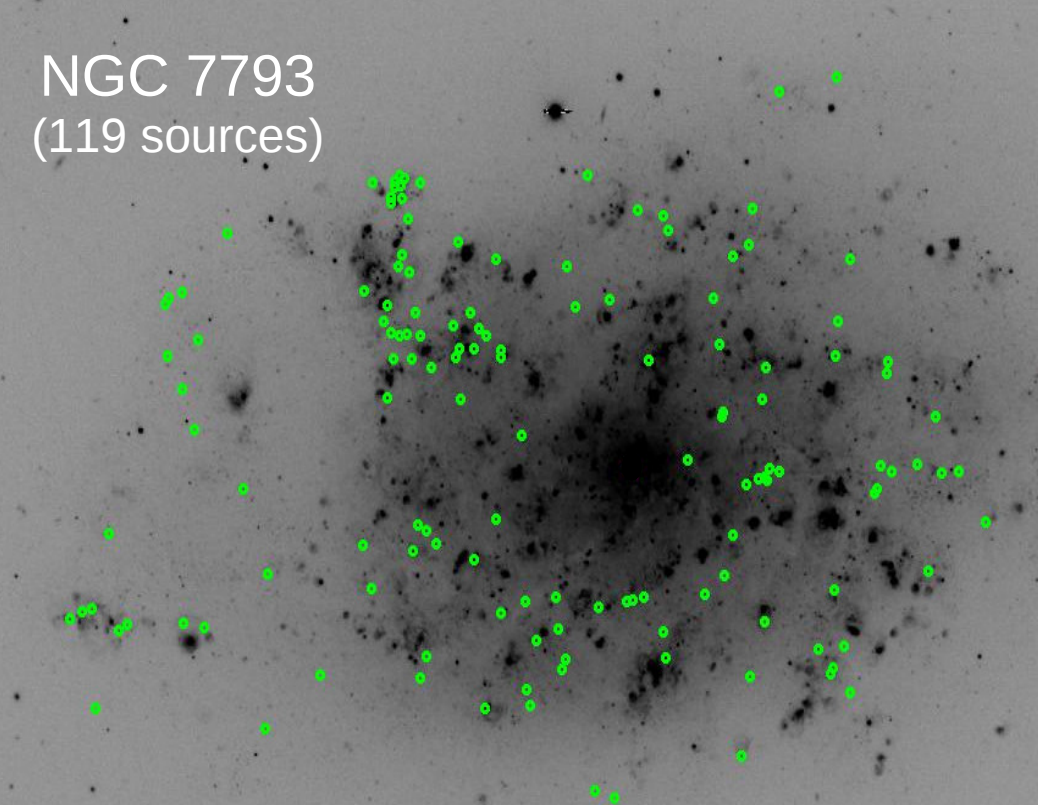
IRAF for photometry

Automated SNR selection

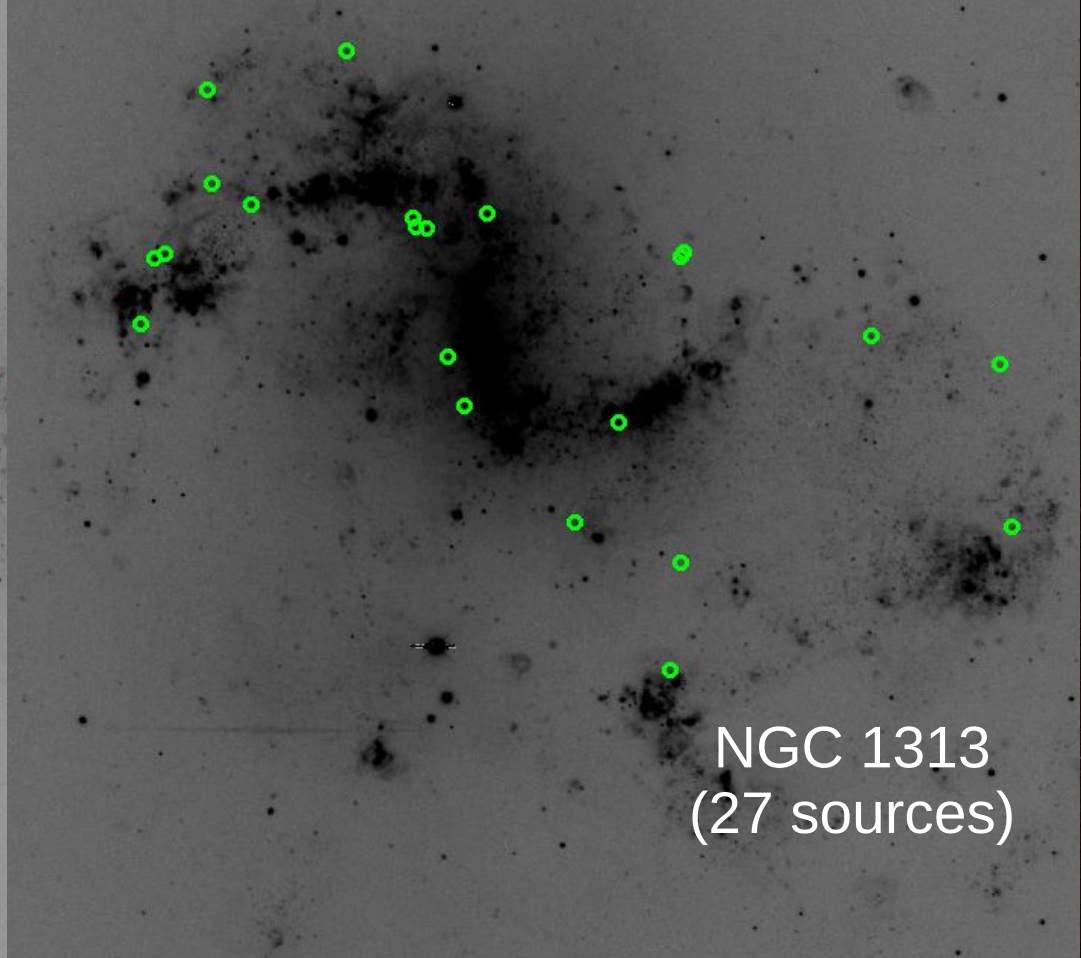
- Continuum subtraction
- Counts $H\alpha > 3\sigma$
- $H\alpha$ excess-magnitude diagram
- $[S II]/H\alpha > 0.4$ (Mathewson & Clarke, 1973)
- In total ~ 180 candidate SNRs (down to 6.5×10^{-17} erg/cm²/s)



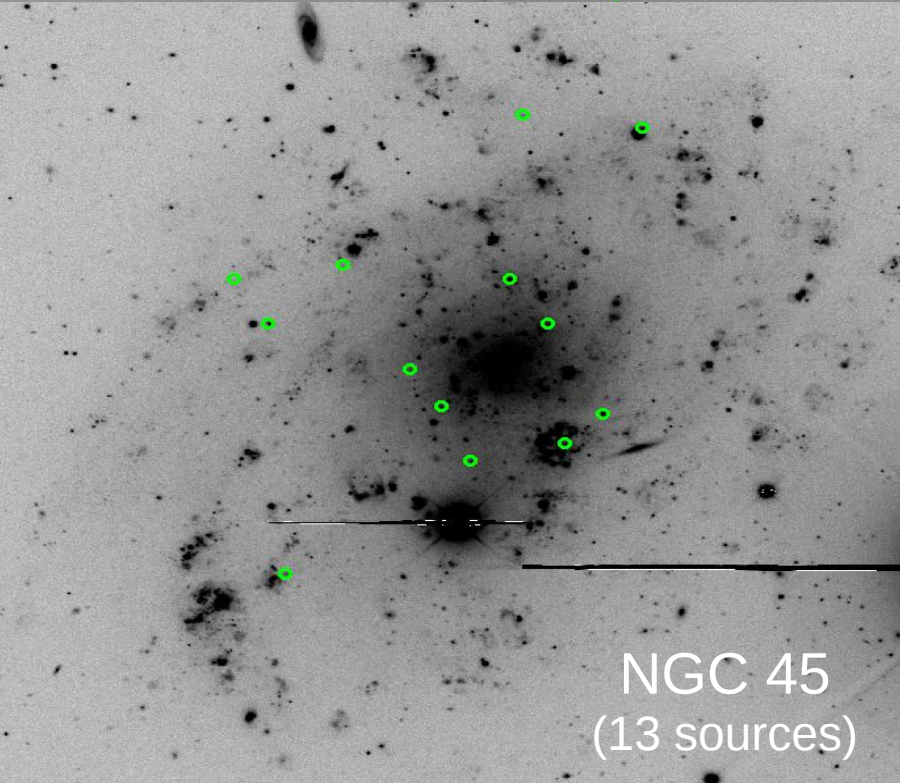
NGC 7793
(119 sources)



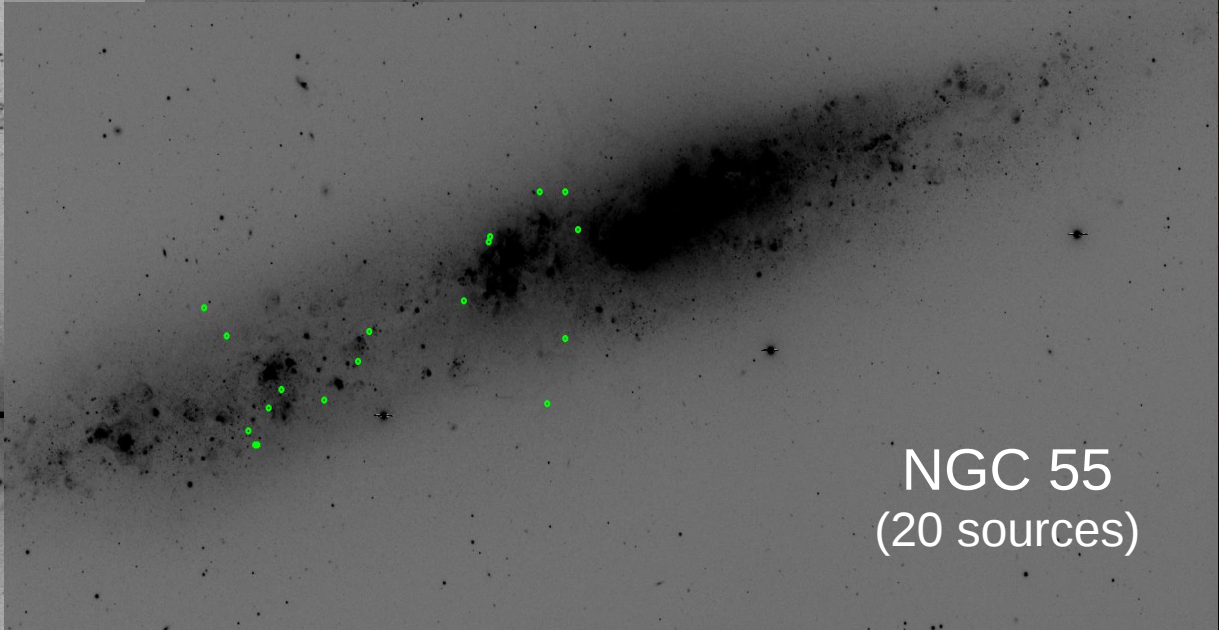
NGC 1313
(27 sources)



NGC 45
(13 sources)



NGC 55
(20 sources)

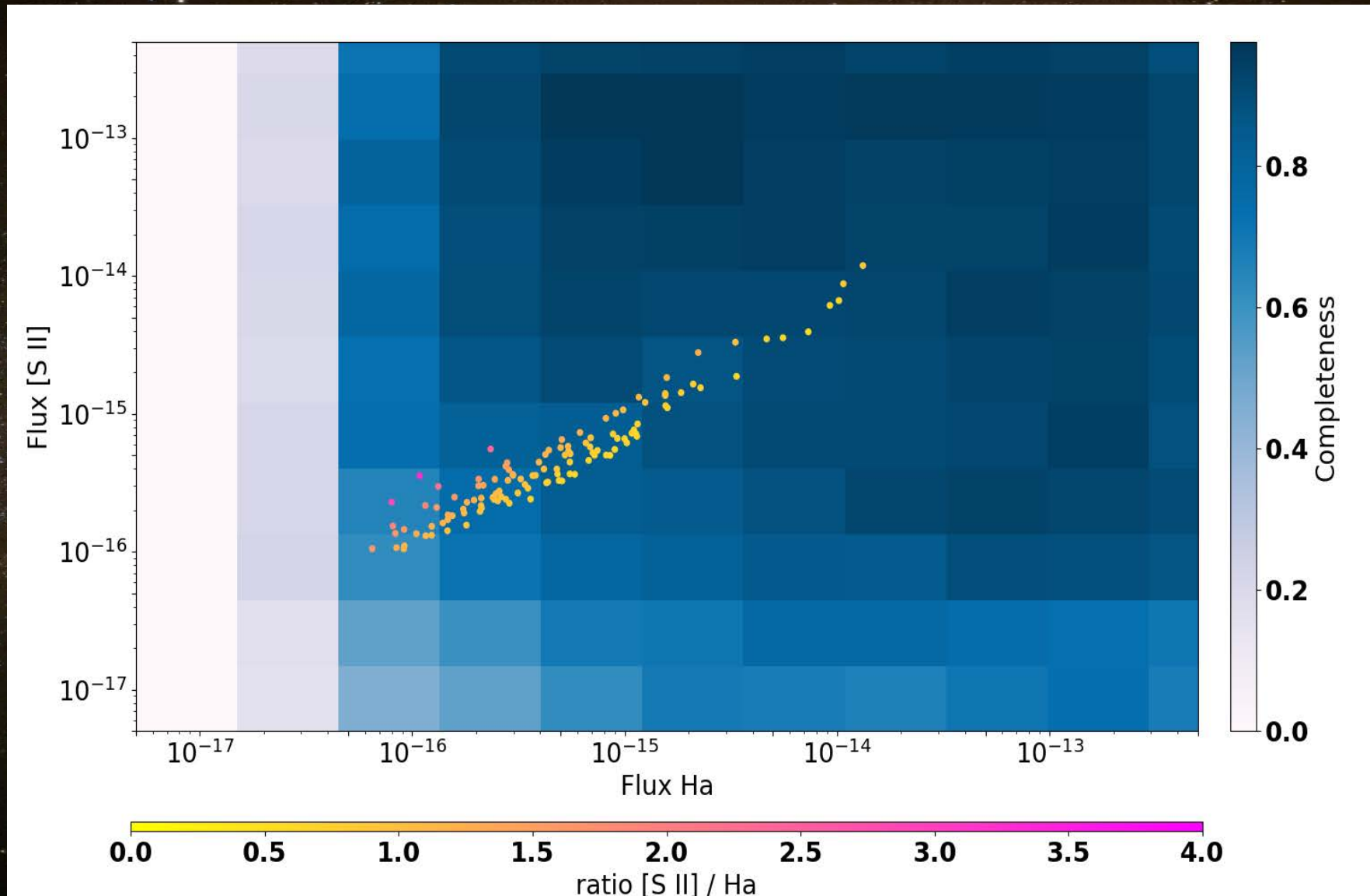


Incompleteness

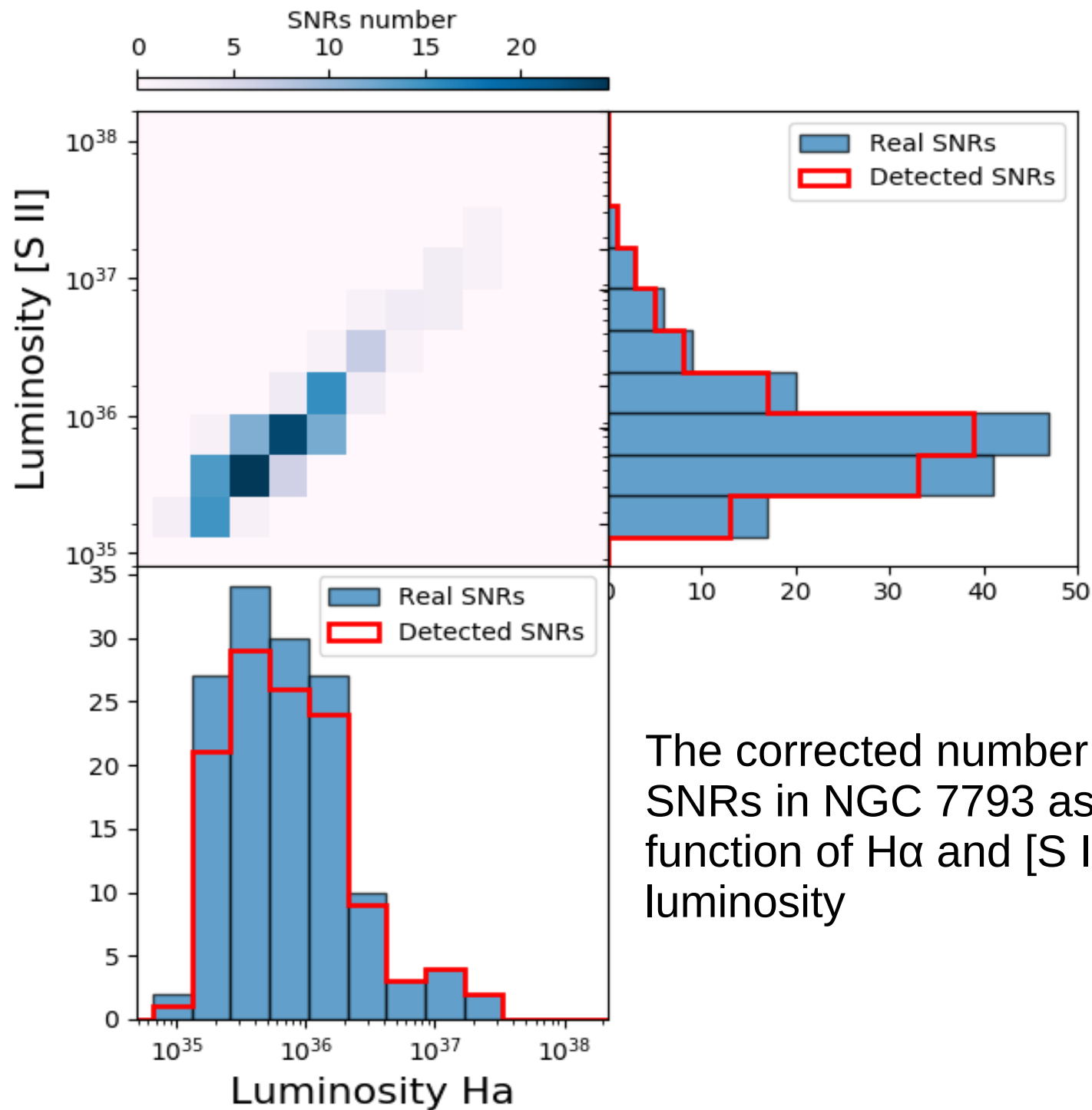
- ▶ Automated process for SNR detection
 - Creation of artificial objects using the PSF of each image
 - Same process with artificial objects
 - Incompleteness map
 - Luminosity function

Incompleteness map for NGC 7793

The two-dimensional completeness map shows the fraction of SNRs that we are able to detect as function of their H α and [S II] flux.

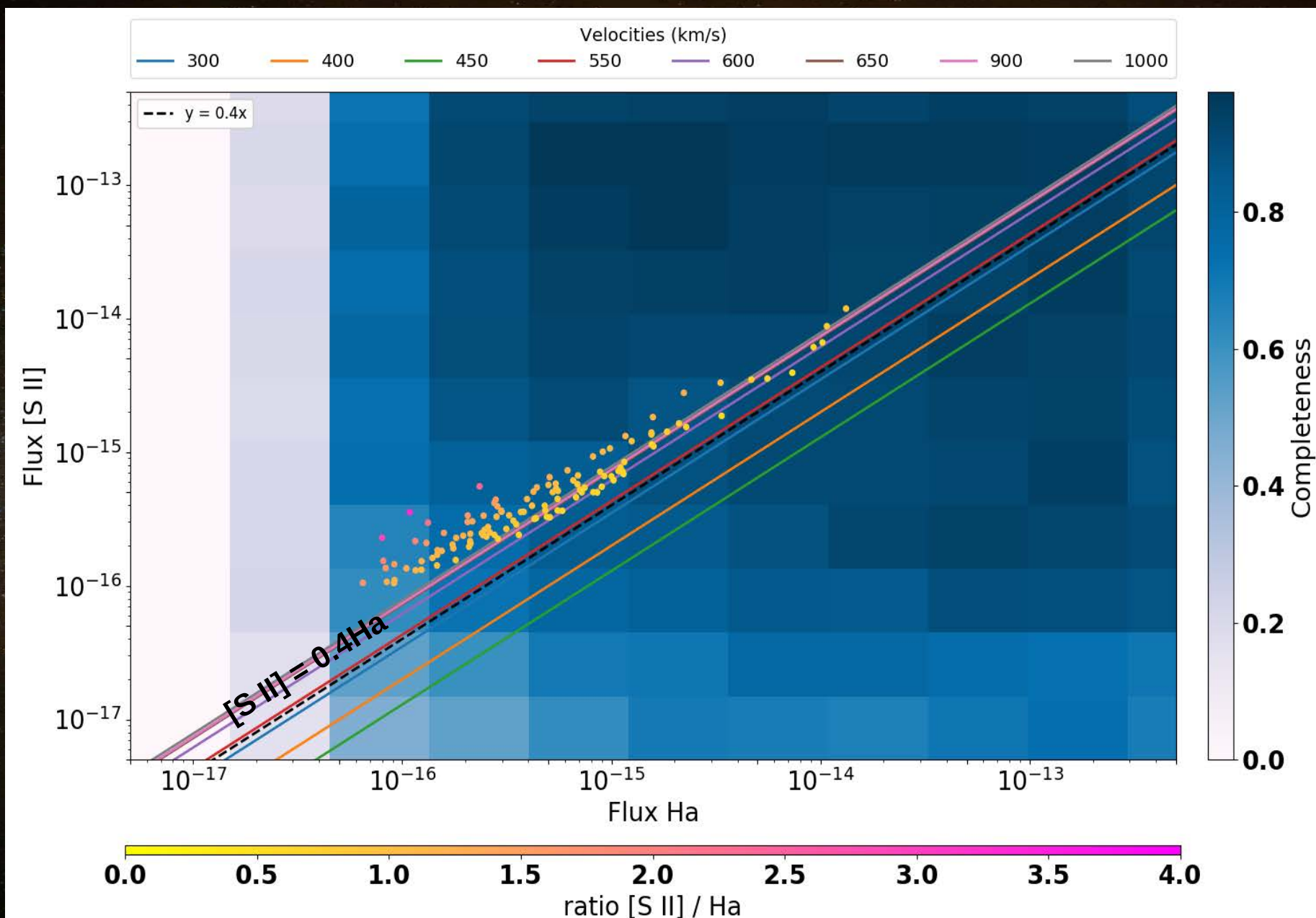


(Kopsacheili et al. 2019, in prep.)



The corrected number of SNRs in NGC 7793 as function of $H\alpha$ and [S II] luminosity

Incompleteness map for NGC 7793 – shock velocities



(shock models from Allen et al. 2008)

Shock and photoionization models

MAPPINGS III: (Groves et al. 2004; Dopita et al. 2002; Sutherland & Dopita 1993; Binette et al. 1984)

- Shock models (Allen et al. 2008)

Velocity (V): 100 - 1000 km/s

Magnetic parameter ($B/n^{1/2}$): $10^{-4} - 10\mu\text{Gcm}^{3/2}$

Density (n): 0.01, 0.1, 1.0, 10, 100, 1000 cm^{-3}

Abundance: LMC, SMC, solar, 2xsolar

- Photoionization models (Kewley et al. 2001; Fioc & Rocca-Volmerange 1997; Leitherer et al. 1999; Levesque et al. 2010, Vázquez & Leitherer 2005)

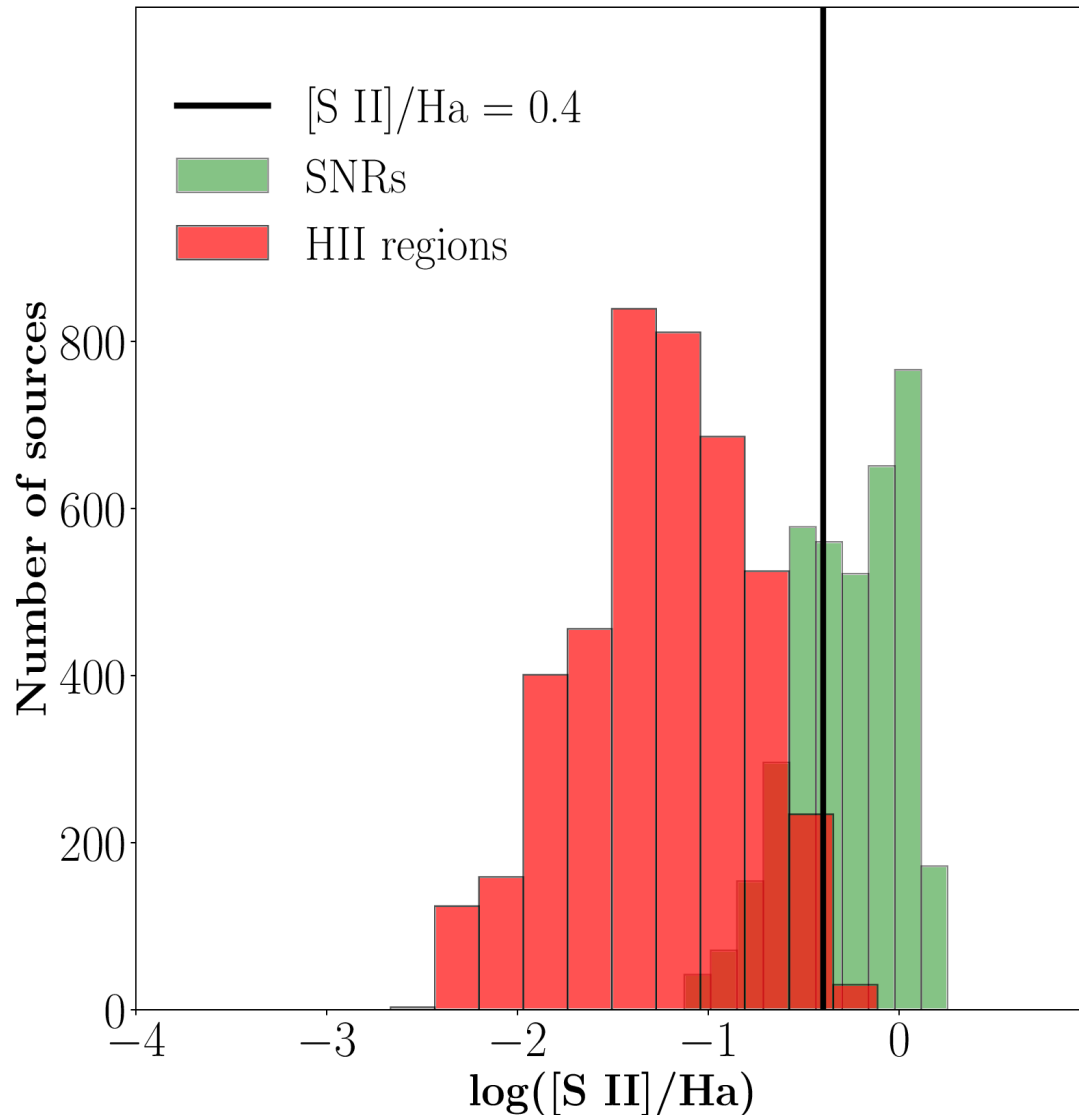
Ionization parameter (Q): $2 \times 10^5 - 4 \times 10^8$

Metallicity (Z): $0.01 - 3Z_{\odot}$

Age: 0 - 10 Myr

Density (n): 10, 100, 350 cm^{-3}

[S II]/H α ratio for photoionized and shock-excited regions

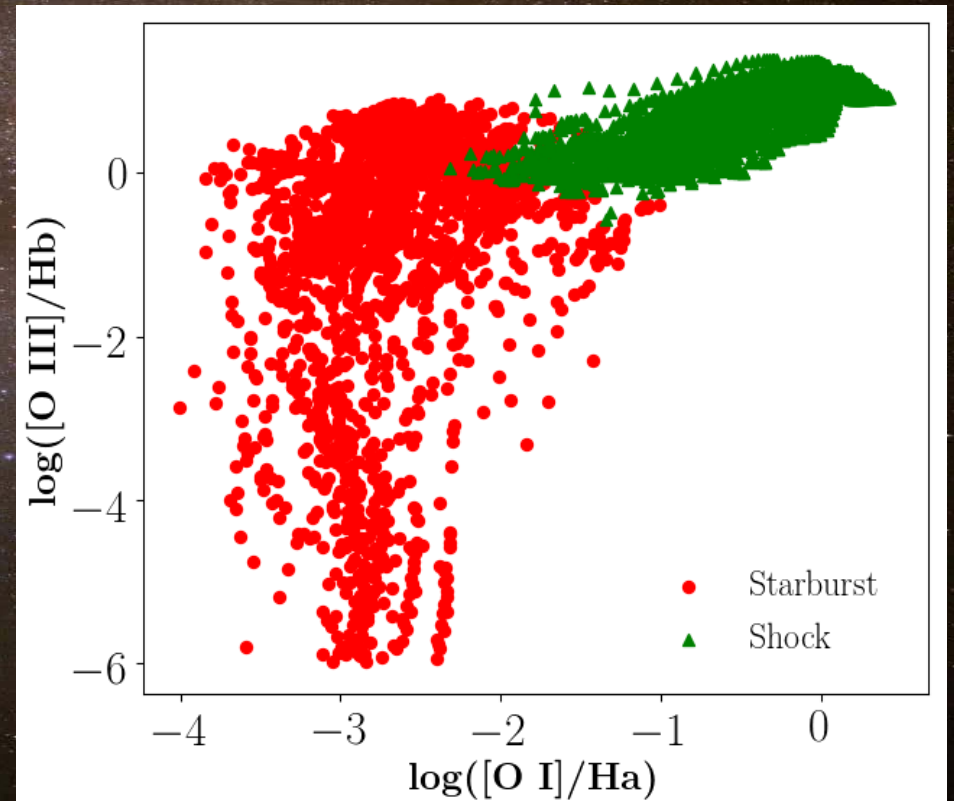
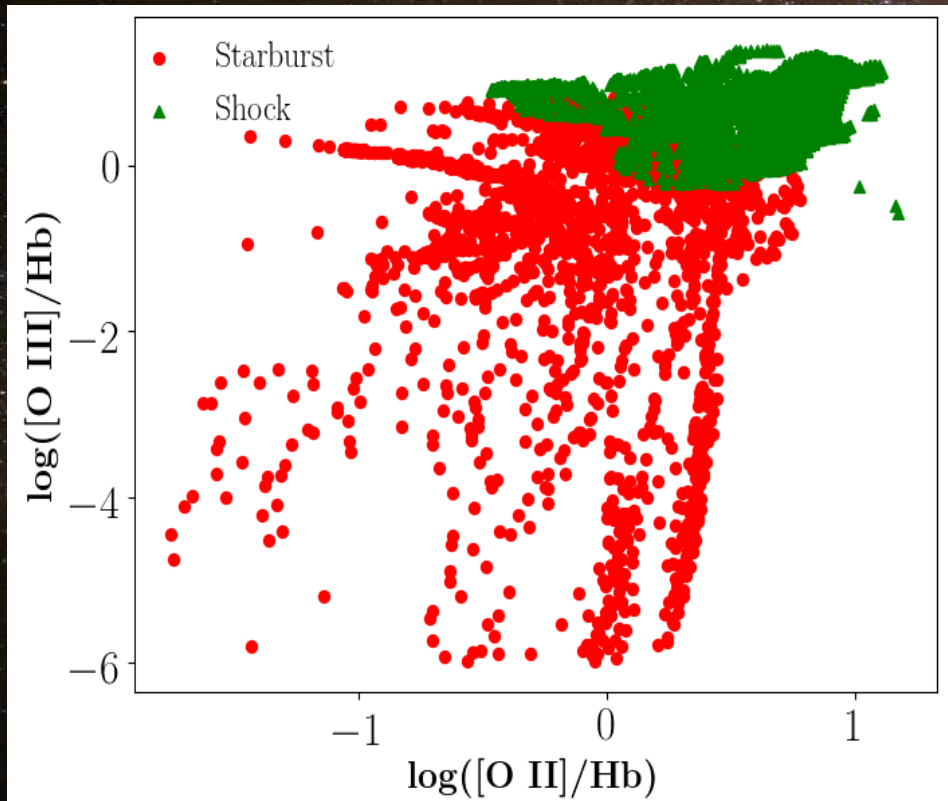


- ◇ MAPPINGS III models
- ◇ Photoionized regions \rightarrow HII regions
- ◇ Shock-excited regions \rightarrow SNRs

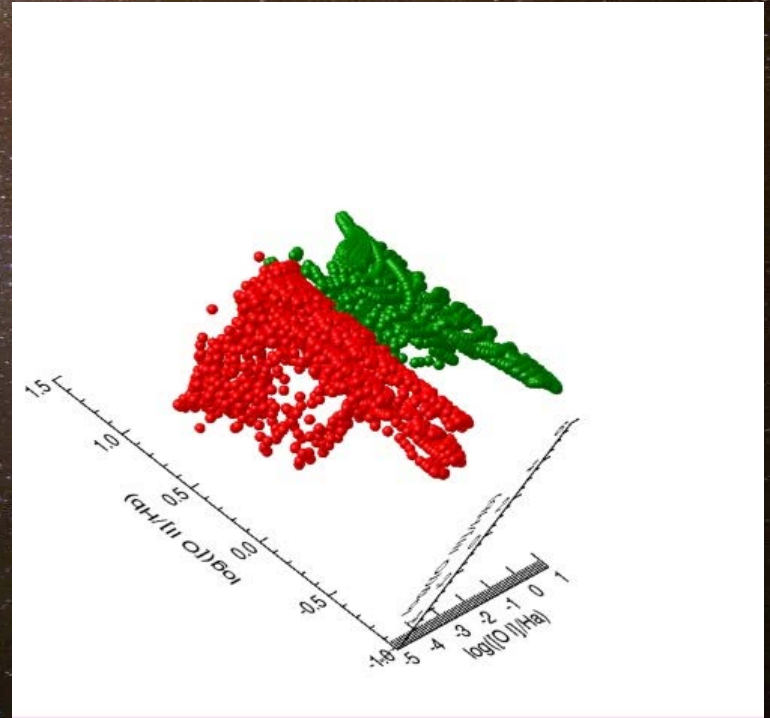
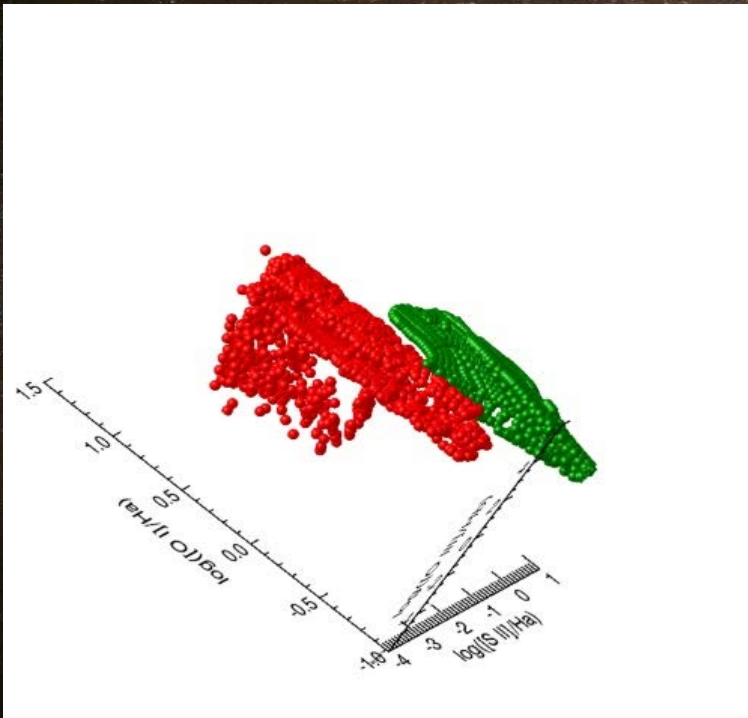
- ◆ Significant fraction of SNRs with $[\text{S II}]/\text{H}\alpha < 0.4$
- ◆ Contamination by HII regions
Need to reconsider the traditional SNR diagnostic

[N II]($\lambda 6583$),
[S II]($\lambda\lambda 6716, 6731$),
[O I]($\lambda 6300$), [O III]($\lambda 5008$)
[O II]($\lambda\lambda 3727, 3729$)

2D diagnostics



3D diagnostics



Support Vector Machine (SVM)

- Classification method
- Separation line (2D) or surface (3D)
- Decision function – Kernel

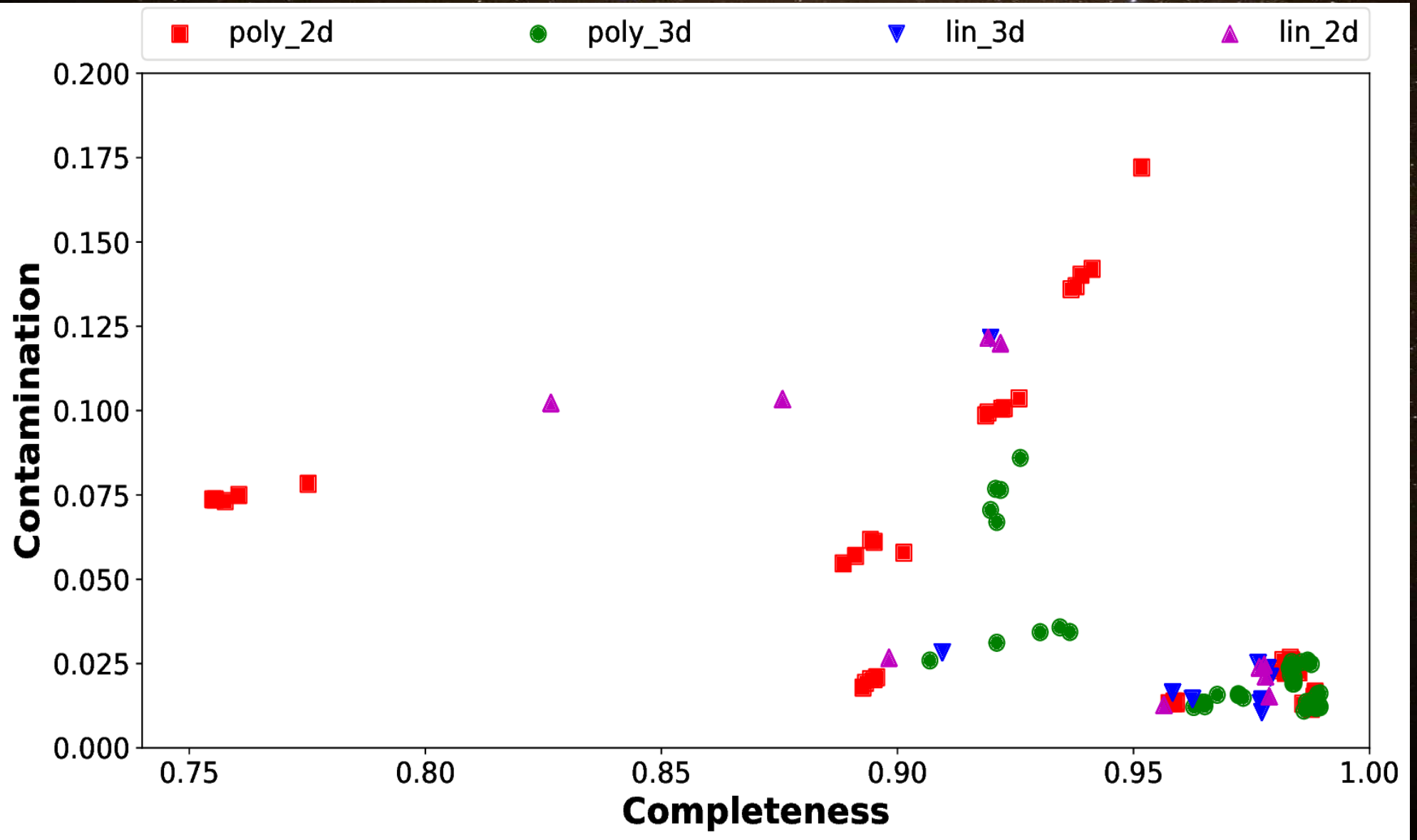
$$K(x^T, x_i) = (\gamma \langle x, x_i \rangle + r)^d,$$

where γ is the kernel width parameter, x_i are the support vectors, r is a constant coefficient, which in our case equals to 1, and d is the degree of the polynomial.

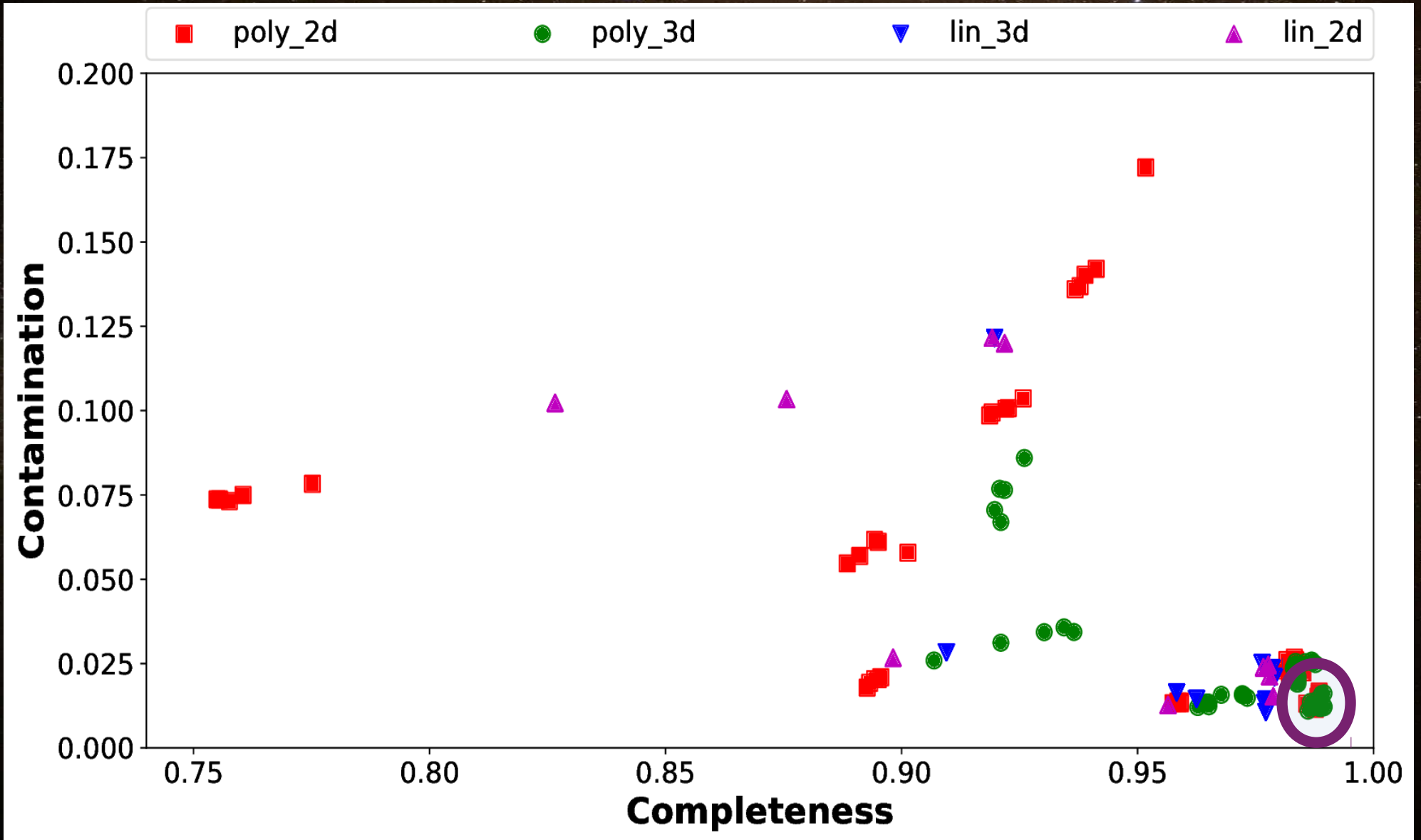
$d = 1$ (linear kernel), 3 (polynomial kernel of 3rd degree)

$\gamma = 0.2 - 1.0$

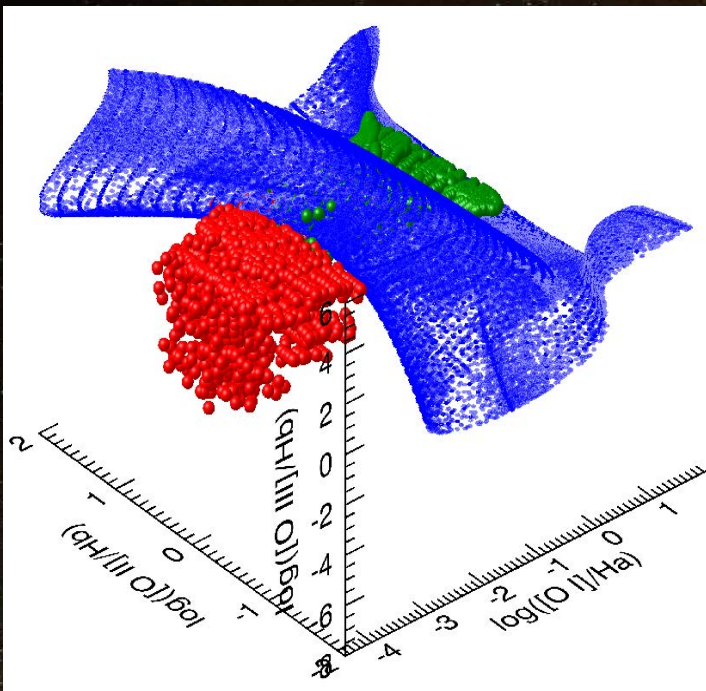
Completeness of SNRs = true positives / (true positives + false negatives)
Contamination of SNRs = false positives / (true positives + false positives)



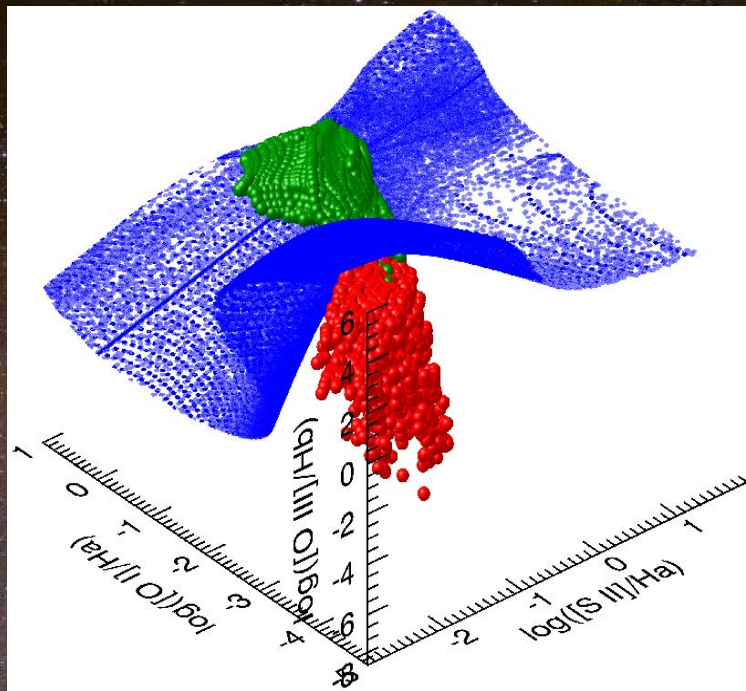
Completeness of SNRs = true positives / (true positives + false negatives)
Contamination of SNRs = false positives / (true positives + false positives)



3D diagnostics



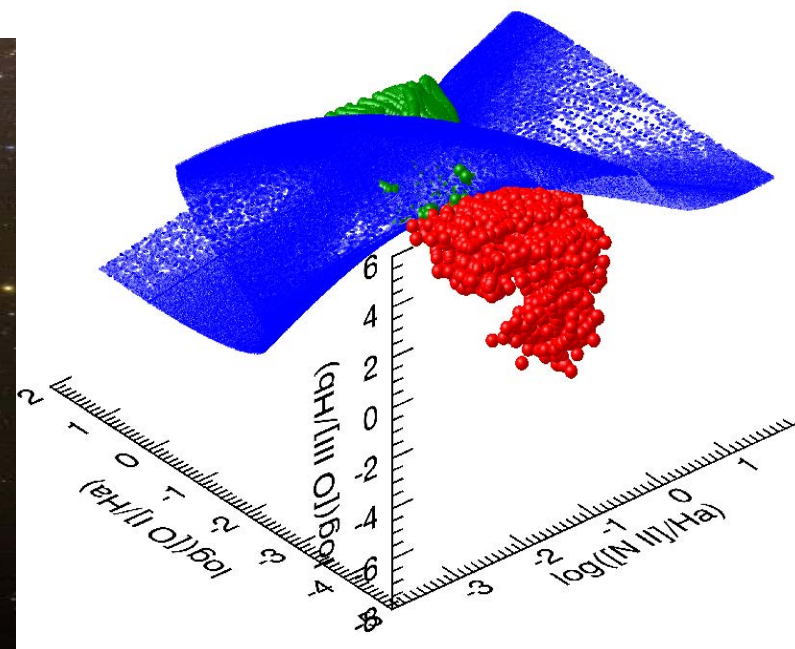
a



b



c



a

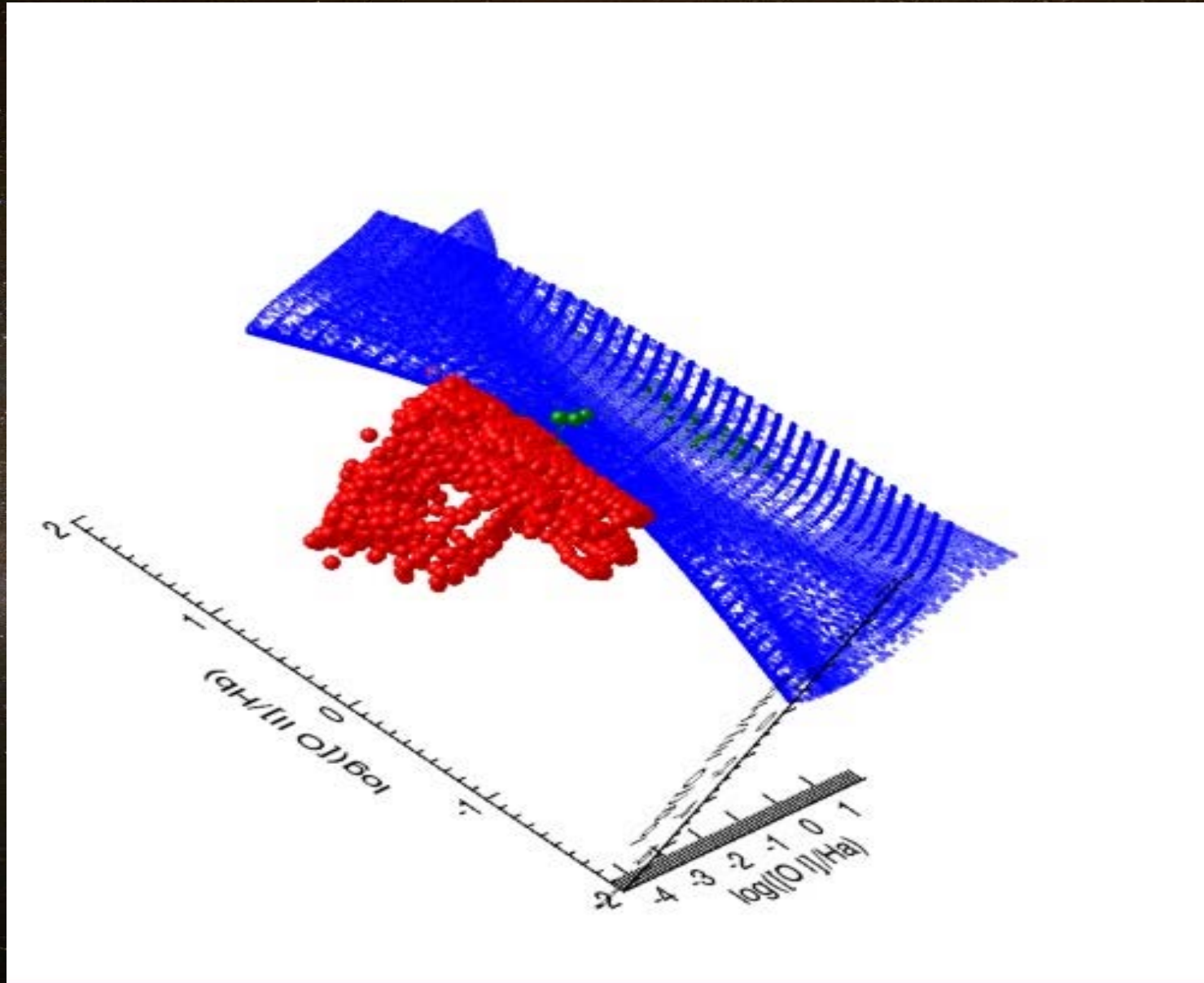
b

c

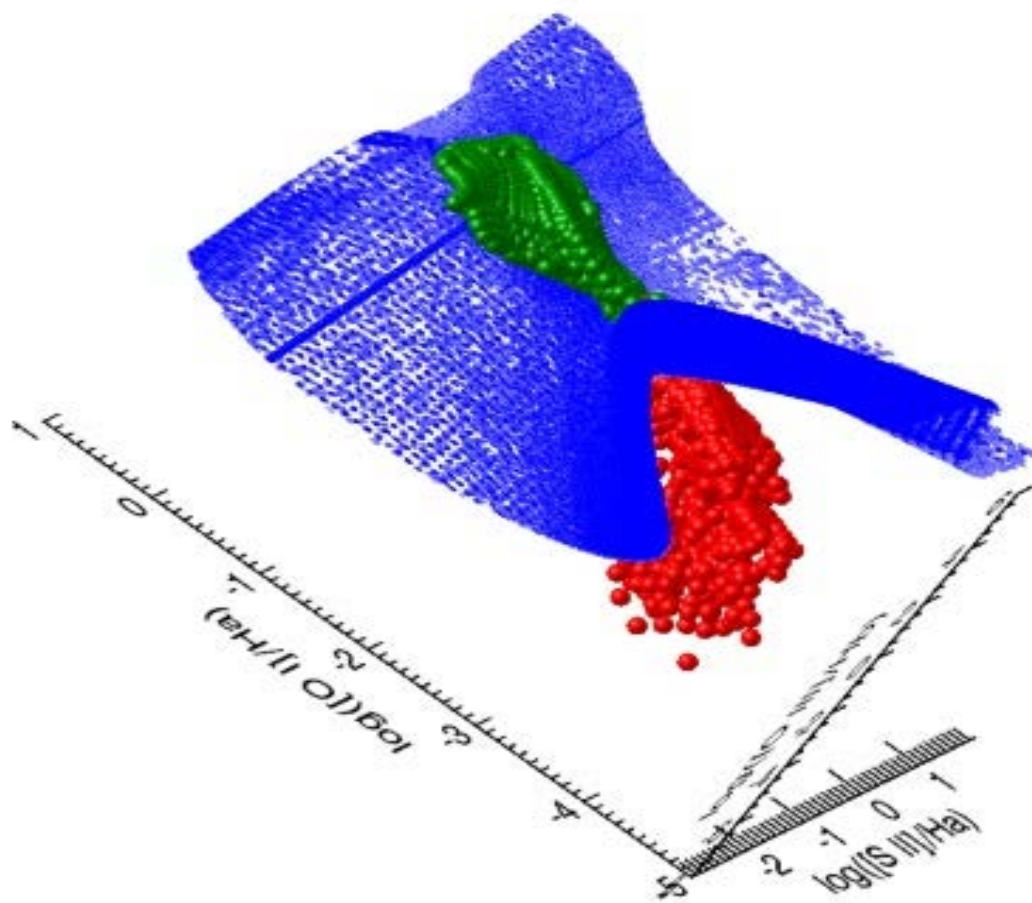
Completeness: 0.9895 0.9895 0.9885
 Contamination: 0.0120 0.0162 0.0121

(Kopsacheili et al., 2019, MNRAS, submitted)

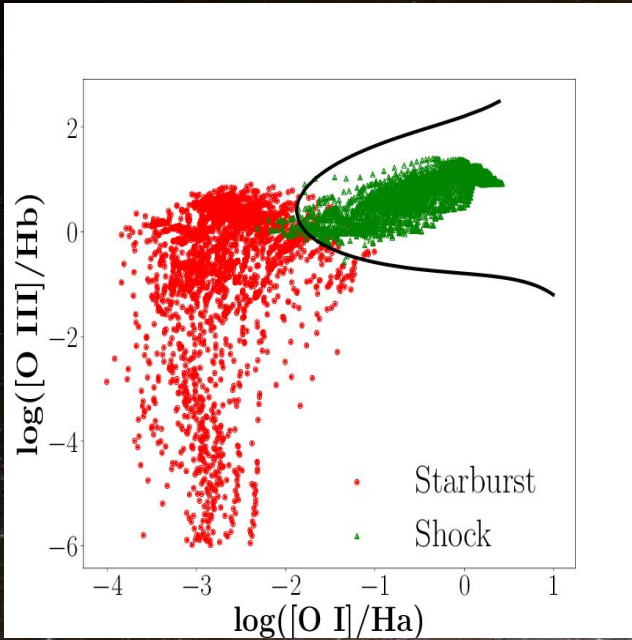
$[O\ I]/H\alpha - [O\ II]/H\beta - [O\ III]/H\beta$



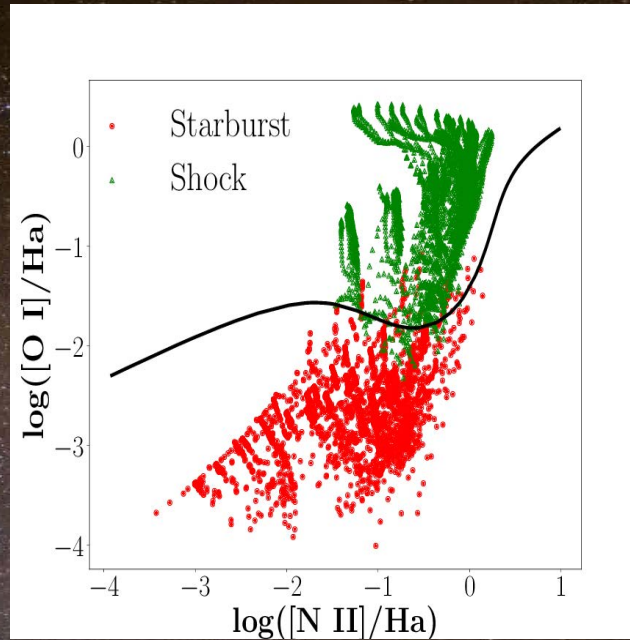
$[S II]/H\alpha - [O I]/H\alpha - [O III]/H\beta$



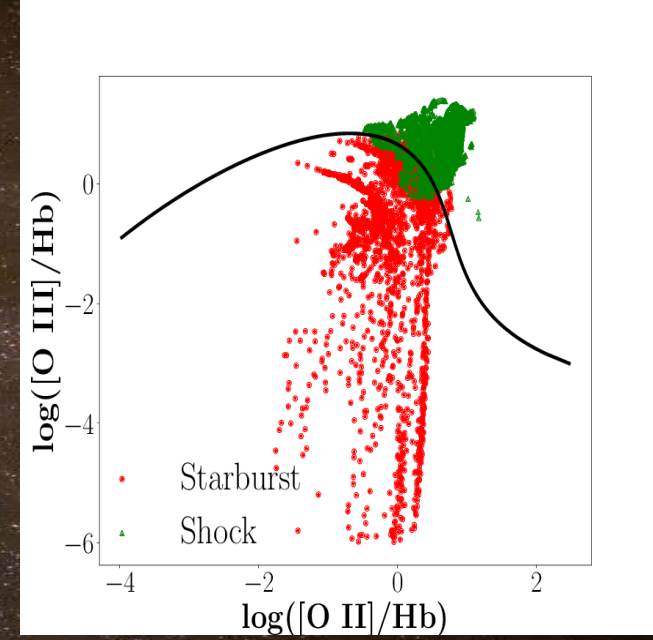
2D diagnostics



d



e



f

d

e

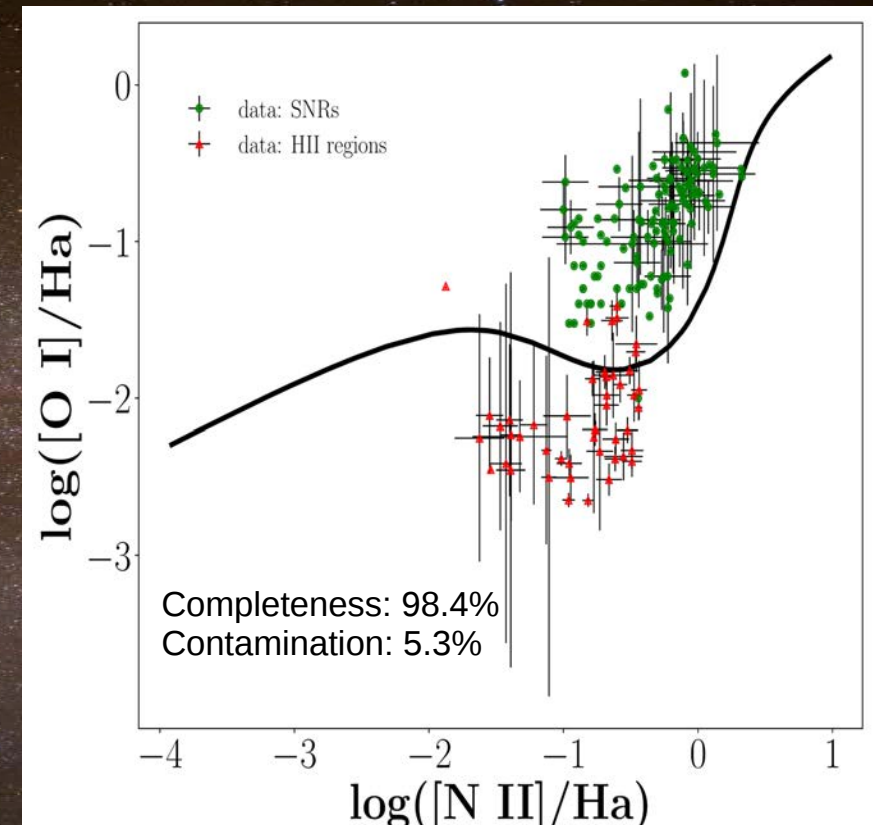
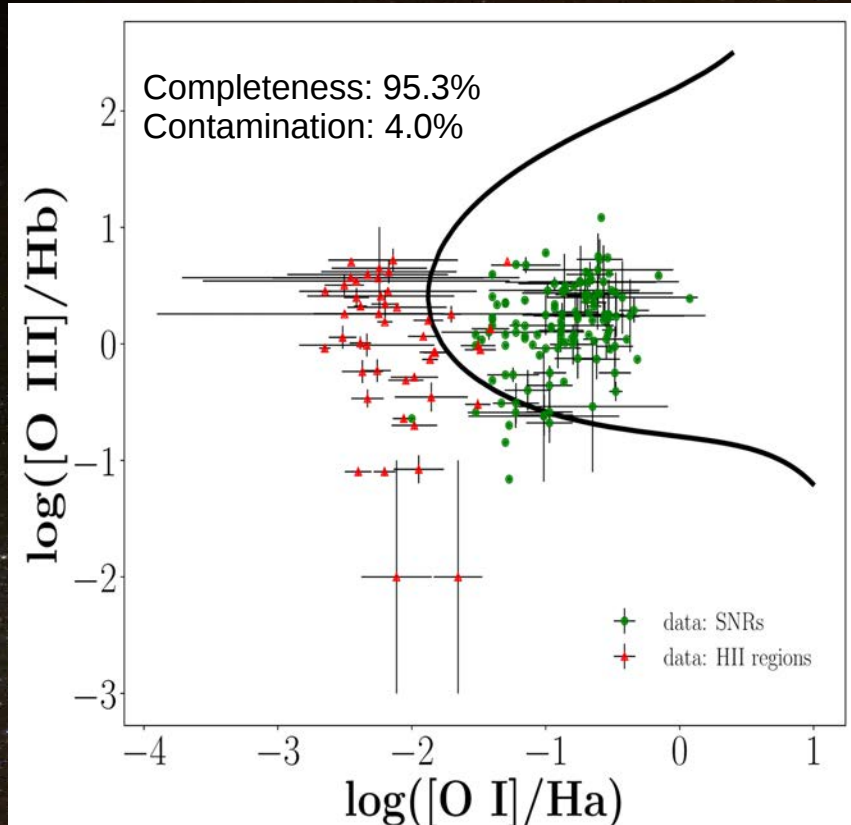
f

Completeness: 0.9877 0.9832 0.9014

Contamination: 0.0116 0.0232 0.0579

(Kopsacheili, M. et al., 2019, MNRAS, submitted)

Compare real data



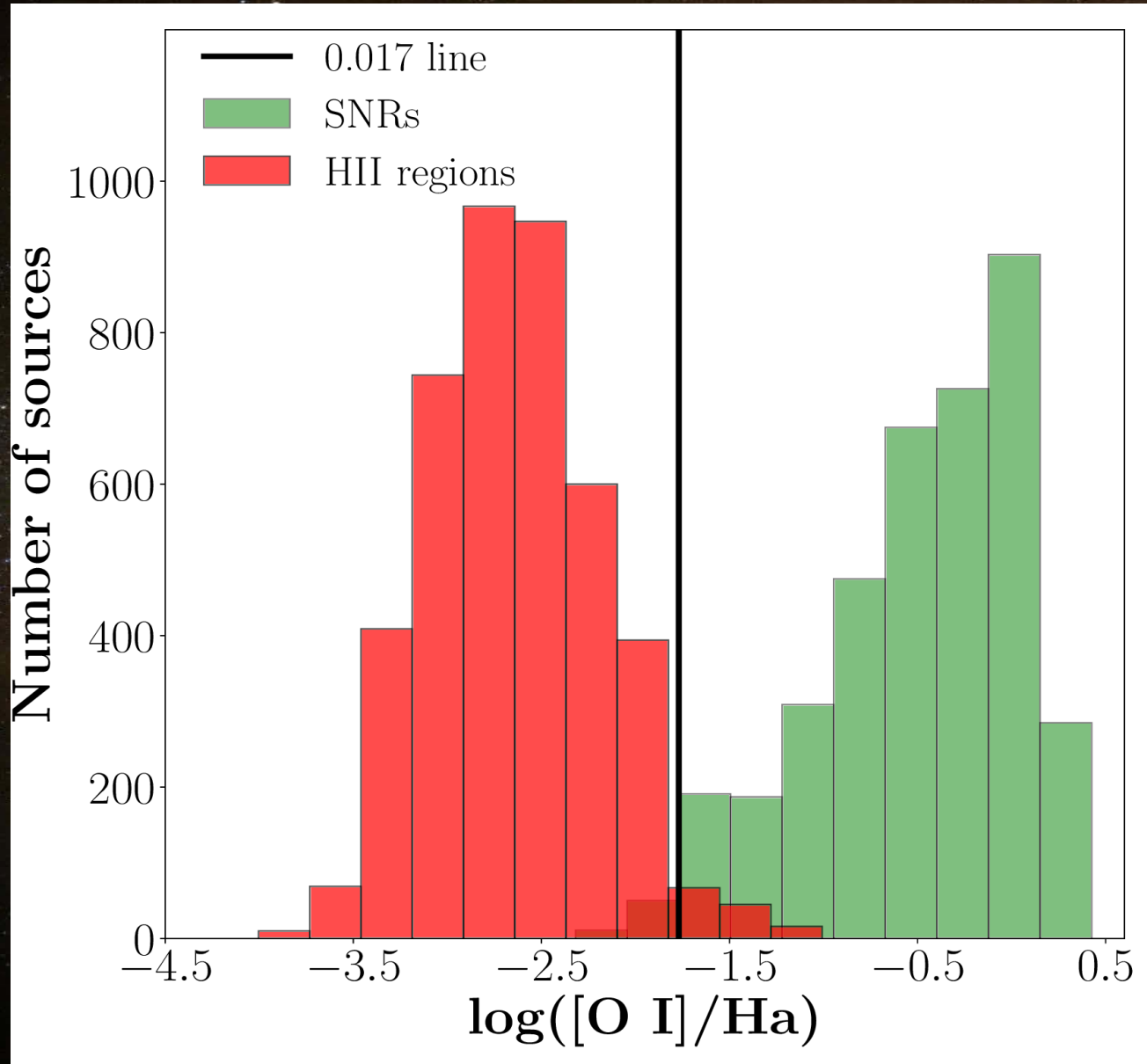
HII regions:

Zurita & Bresolin, 2012;
Bresolin, 2007; Tsamis, 2003;
Castellanos et al., 2002;
Vílchez & Esteban, 1996;
Russel & Dopita, 1990; Kwitter
& Aller, 1980; Dufour, 1975

SNRs:

Long et al., 2019;
Lee et al. 2015;
Leonidaki et al., 2013;
Matonick & Fesen, 1997

More effective 1D diagnostic



Completeness: 97.2%
Contamination: 2.4%

Summary

- SNR detection using an automated way
- Use of artificial objects in order to quantify incompleteness maps and construct Luminosity Functions
- New 2D and 3D diagnostics for SNR classification
- Introduce a 1D diagnostic ($[\text{O I}]/\text{H}\alpha > 0.017$) sensitive to lower velocity SNRs.

A night sky photograph featuring the Milky Way galaxy. The galaxy's core is visible as a bright, dense band of stars, stretching from the upper left towards the center. The sky transitions from a deep purple and blue at the top to a dark red and orange glow near the horizon, likely due to light pollution or the setting sun. In the foreground, a dark, silhouetted landscape is visible, including a body of water on the left and a line of trees on the right. The overall scene is serene and awe-inspiring.

Thank you!